

Simple Synthetic Manipulation Allowing for Morphological Diversity of Porphyrin-Based Microcrystals

Jun Ho Lee, Eui-Hyun Ryu, Sungtae Kim, and Suk Joong Lee*

Department of Chemistry, Korea University, Seoul 136-701, Korea. *E-mail: slee1@korea.ac.kr

Received October 28, 2010, Accepted December 13, 2010

Amphiphilic (porphyrin)Sn(OH)₂ molecular building block can directly translate into well-defined solid-state micro-crystalline structures. The crystalline diamond plates are obtained from ethanol and crystalline square plates are grown from methanol solution. With a simple synthetic manipulation during the microcrystal growth, the morphologies can be controlled by adopting different molecular packing. Consequently, morphologies of microcrystals have been diversified. Furthermore, the macroscopic crystals were obtained in the presence of cetyltrimethylammonium bromide (CTAB).

Key Words: Amphiphilic, Porphyrin, Building block, Nanocrystalline, CTAB

Introduction

Over the past decade self-assembly approach has become one of the most powerful techniques for synthesis of nanostructures.¹ This self-assembly approach is spontaneous processes via dynamic noncovalent interactions such as van der Waals, π-π, hydrogen bonding, hydrophilic/hydrophobic, electrostatic, donor and acceptor, and metal-ligand coordinations between the building blocks.² Particularly, porphyrins have become one of the most attractive building blocks for self-assemblies because of the enormous potentials in catalysis, photochemistry, sensing, and optical devices which have made them favorite building blocks in the emerging field of molecular materials.³ Depending on suitable substituents, porphyrin can promote a variety of noncovalent interactions and produce vastly diverse nanostructures including spheres, rods, wires, ribbons, tubes, and fibers.⁴

The investigations on the fabrication and preparation of diverse porphyrin nanostructures are best relying upon reaction conditions. One common method to manipulate nanostructure shape is to utilize a growth medium containing precursors that adopt preferentially on certain crystalline packing.⁵ The final morphologies of nanocrystals are mainly determined by surface energy and diffusion rate that permit crystal growth rate, direction and final morphology to be controlled.⁵ In other words, the achievement of nanostructure assemblies and their morphology controls is often depending on the reaction temperatures and choice of solvents. We are particularly interested in the rational synthesis of porphyrin based unique nanostructures showing a variety of morphology by manipulating reaction temperatures and solvents to engender various interactions between the porphyrin building blocks which may diversify the morphology of nanostructures. Therefore, we report here the synthesis and characterization of various micro crystalline structures with 5,15-bis(pyridyl)-10,20-diarylporphyrin]Sn(OH)₂ as a building block from different crystal growth conditions. With the variation of reaction temperatures and solvents (ethanol and methanol), this amphiphilic (porphyrin)Sn(OH)₂ can easily adopt various microcrystalline plates with a tunable size and shape.

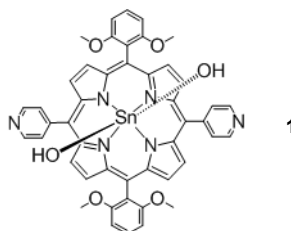
The structural feature of the microcrystalline plates was characterized by scanning electron microscopy (SEM) and powder X-ray diffraction (PXRD). Furthermore, the size of the plates can grow into macroscopic crystalline films through the simple surfactant assistance.

Experimentals

General. All chemicals were obtained from commercial sources and used without further purification. 5,15-Bis(4-pyridyl)-10,20-[2,6-di(*n*-methoxy)phenyl]porphyrin and [5,15-Bis(4-pyridyl)-10,20-[2,6-di(*n*-methoxy)phenyl]porphyrinato]tin(IV) dihydroxide (1) were synthesized according to modified literature procedures.^{6,7} All other chemicals were obtained from commercial sources and used without further purification. All of the reactions were carried out under N₂ with the use of standard N₂-atmosphere and Schlenk techniques unless otherwise noted. NMR spectra were recorded on a Varian AS 400 (399.94 MHz for ¹H and 100.57 MHz for ¹³C) spectrometer. Absorbance and emission spectra were obtained using a Agilent P453 UV-vis spectrophotometer and a Hitachi F-7000 fluorescence spectrophotometer using quartz cells. Matrix-assisted laser-desorption-ionization time-of-flight mass spectra (MALDI-TOF) were obtained on a PE Voyager DE-Pro MALDI-TOF Mass Spectrometer in the Analytical Services Laboratory at Northwestern University. All scanning electron microscopy (SEM) images were obtained using a Jeol JSM-7500F in Basic Science Institute at Sungshin Women's University, Seoul, Korea. Powder X-ray diffraction measurements were recorded with a Rigaku D/MAX-Ultima III diffractometer using nickel-filtered Cu Kα radiation ($\lambda = 1.5418 \text{ \AA}$) over a range of $5^\circ < 2\theta < 65^\circ$ and an X'Celerator detector operating at 40 kV and 40 mA.

Synthesis.

[5,15-Bis(4-pyridyl)-10,20-[2,6-di(*n*-methoxy)phenyl]porphyrinato]tin(IV) Dihydroxide (1):^{6,7} A solution of 5,15-Bis(4-pyridyl)-10,20-[2,6-di(*n*-methoxy)phenyl]porphyrin which was synthesized according to literature procedures⁷ (0.17 mmol) and SnCl₂·2H₂O (340 mg, 1.7 mmol) in pyridine (15 mL) were refluxed under air with exclusion of light for 4 h. After cooling,

**Scheme 1**

water (60 mL) was added, and the dark red precipitate was collected by filtration which was further dissolved in THF (125 mL). To the porphyrin solution, K_2CO_3 (2.75 mmol) and water (30 mL) were added. The resulting mixture was refluxed for 6 h. After washing with water, the organics was purified by alumina column chromatography ($CHCl_3/MeOH$ 95.5:0.5 v/v) to afford the **1** as a dark purple solid (151 mg, 89% yield). 1H NMR ($CDCl_3$) δ 9.13 (d, $^3J_{H-H} = 4.4$ Hz, 4H), 9.08 (d, $^3J_{H-H} = 5.1$ Hz, 4H), 9.06 (d, $^3J_{H-H} = 4.4$ Hz, 4H), 8.32 (d, $^3J_{H-H} = 5.1$ Hz, 4H), 7.84 (t, $^3J_{H-H} = 8.8$ Hz, 2H), 7.09 (d, $^3J_{H-H} = 8.8$ Hz, 4H), 3.58 (s, 12H). $^{13}C\{^1H\}$ NMR ($CDCl_3$) δ 160.43, 149.59, 148.63, 147.57, 145.63, 132.70, 132.43, 131.60, 129.92, 117.88, 117.37, 114.39, 104.41, 56.19. MS (MALDI-TOF) m/z 872.0 for $[M-OH]^+$; Calcd 870.52.

Synthesis of Porphyrin Microcrystals: An alcoholic solution of porphyrin (100 μ L of a 1 mM solution) was injected into a vial containing stirring deionized water (5 mL) at 45 $^{\circ}$ C or 90 $^{\circ}$ C. Stirring was maintained for approximately 1 to 10 min until colloidal porphyrin particles were obtained. Isolation of all porphyrin microcrystals after synthesis was easily carried out via centrifugation and decantation of the mother liquor.

Results and Discussion

Previously, Hupp and co-workers⁷ have reported the effect of secondary substituent on porphyrin based nanoparticles morphologies. They have demonstrated the manipulation of secondary substituents that are not directly bonded to the porphyrin ring to lead van der Waals interactions affecting significantly the morphologies of the nanoparticles. We have envisaged that simple changes in the van der Waals surfaces of the building blocks by using in different growth mediums would affect the molecular packing during the nanostructure syntheses.

Using the Shelnutt and other's reprecipitation methods,⁸ when an ethanolic solution of **1** is injected into stirring water at 45 $^{\circ}$ C, a light brown suspension is obtained. Collections of fairly uniform hexagonal plates that are 2 - 3 μ m long (Fig. 1a) are identified by scanning electron microscopy (SEM) analysis. Furthermore, when a solution of **1** in ethanol is injected into stirring water at 90 $^{\circ}$ C, diamond plates with 10 μ m long are obtained (Fig. 1b). As reaction temperature increased, the size of porphyrin microcrystals is increased. Interestingly, when a methanolic solution of **1** is injected into stirring water at 45 $^{\circ}$ C, a light brown suspension is also obtained which is appeared to be a collection of diamond plates with 10 μ m long (Fig. 1d). These diamond plates resemble closely to the microcrystals grown in ethanol at 90 $^{\circ}$ C (Fig. 1b), although they have pre-

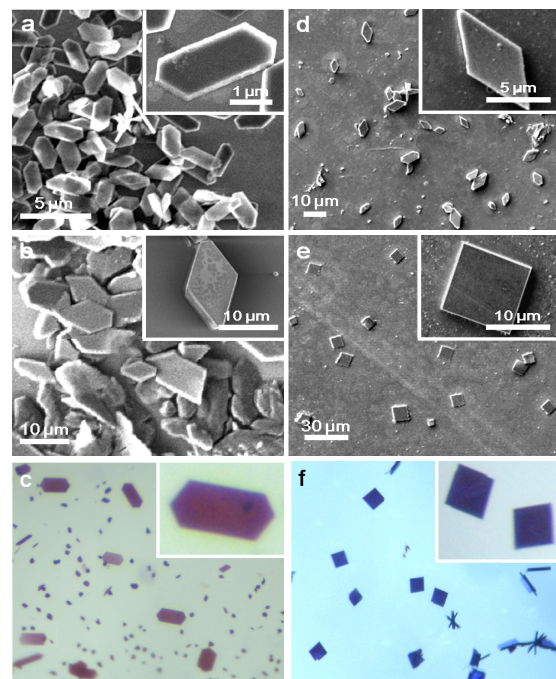


Figure 1. SEM (a, b, d and e) images of the different microcrystal morphologies and optical microscopic (c and f) images of single crystals obtained from porphyrin building block **1**. Conditions; a) and d): 45 $^{\circ}$ C, stirring; b) and e): 90 $^{\circ}$ C, stirring; c) and f): rt, non-agitated slow diffusion.

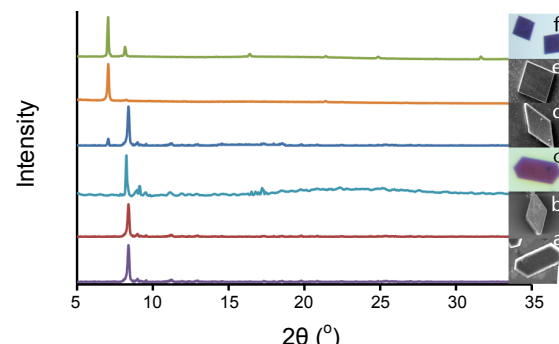


Figure 2. The PXRD patterns for the microcrystal samples (a, b, d and e) as well as that obtained for a single-crystal samples (c and f) of **1**. a) Hexagonal plates grown with EtOH under stirring at 45 $^{\circ}$ C. b) Diamond plates grown with EtOH under stirring at 90 $^{\circ}$ C. c) Single crystal grown with EtOH under non-agitated conditions. d) Diamond plates grown with MeOH under stirring at 45 $^{\circ}$ C. e) Square plates grown with MeOH under stirring at 90 $^{\circ}$ C. f) Single crystal grown with MeOH under non-agitated conditions.

pared in methanol. Remarkably, when a solution of **1** in methanol is injected into water at 90 $^{\circ}$ C, square plates with ~10 μ m long are obtained (Fig. 1e). The morphology has been tuned from diamond plates to square plates. Furthermore, the shape of single crystals grown from slow diffusion in both ethanol (Fig. 1c) and methanol (Fig. 1f) on water over two weeks of period are remarkably similar to those of microcrystals obtained from ethanol (Fig. 1a) and methanol (Fig. 1e) solution in short period of time. Presumably, different diffusion rates of methanol and ethanol in water are responsible for these dramatic changes in their morphologies.

The two microcrystal samples from **1** in ethanol exhibit powder X-ray diffraction (PXRD) patterns (Fig. 2a and b) that closely resemble the diffraction pattern for a single crystal sample grown in ethanol under non-agitated conditions (Fig. 2c). Such similarities imply that the corresponding unit cells for the three samples are identical and suggest a conservation of the molecular packing arrangement. Due to their morphological similarities, the microcrystals (diamond plates, Fig. 1d) grown in methanol at 45 °C exhibit similar PXRD patterns that closely resemble the diffraction patterns (Fig. 2d) for those samples grown in ethanol. However, in case of the sample grown in methanol at 90 °C, square plates (Fig. 1e), the PXRD pattern is no longer similar. For example, the pattern shows one major peak shifted by 2.3 degrees (Fig. 2e) suggesting that it adopts a different molecular packing arrangement in order to form square plates. This microcrystal sample from methanol shows PXRD pattern that closely resemble the diffraction pattern for a single crystal sample grown in methanol under non-agitated conditions (Fig. 2f). Due to the quality of single crystals obtained under slow diffusion and non-agitated conditions, achieving the structures have been unsuccessful.

As multi-porphyrin materials, the microcrystals obtained from both ethanol and methanol exhibit absorption spectra that differ considerably from that of the monomer (Fig. 3). For

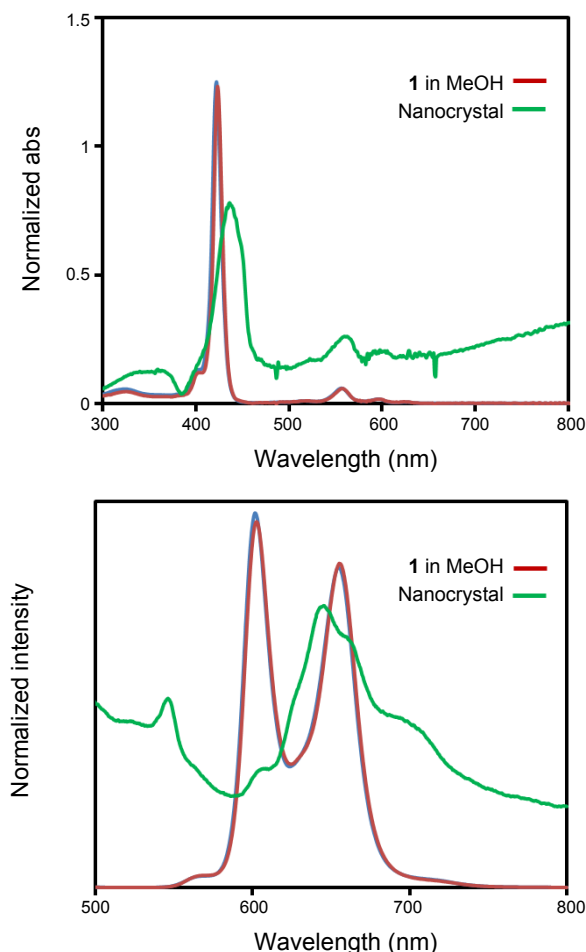


Figure 3. UV-vis and fluorescence spectra of **1** (2.0×10^{-6} M) and microcrystal made from **1**.

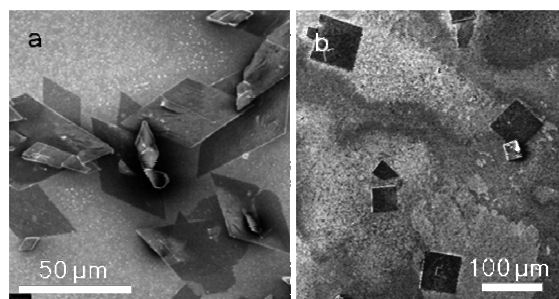


Figure 4. SEM images of macroscopic crystalline thin films assembled in 1 mM aqueous solution of CTAB with ethanolic (a) and methanolic (b) solutions of **1**.

example, compared to monomer **1** in ethanol, which exhibits a Sorét-band at 422 nm with multiple Q-bands around 550 nm, the extinction spectrum of the microcrystal colloidal dispersions on quartz glass plate are more complicated. The Sorét-band is broadened and red-shifted, with sub-peaks at 400 and 433 nm, while the Q-bands red-shift slightly to 560 and 594 nm. Presumably, J-type of packing among porphyrin building blocks is main responsible for these observations. The emission spectrum of the microcrystals shows multiple bands at 602, 642, 661, and 695 nm, while only two bands at 601 and 653 nm are observed for the monomer solution (Fig. 3).

Interestingly, when an ethanolic solution of **1** is injected into solution of cetyltrimethylammonium bromide (CTAB) in water (1 mM) and stirred for 5 min at 90 °C, a light brown suspension is obtained. SEM analysis reveals these porphyrin suspensions as collections of diamond-shaped crystalline thin films with 100 μm long (Fig. 4a). Furthermore, when a solution of **1** in methanol is injected into stirring solution of CTAB in water (1 mM) at 90 °C, square crystalline thin films with 100 μm long is obtained (Fig. 4b). These macroscopic thin films show similar morphologies that have been found during the microcrystals syntheses without the assistance of CTAB.

CTAB is known to form a lamellar phase¹⁰ with hydrophilic channels between the layers of CTABs at high temperature. Presumably, when solutions of **1** are injected into this phase, the amphiphilic porphyrin molecules partition in the channels and self-assemble into crystalline plates. Due to the water in CTAB's lamellar phase, the crystallization occurs in a similar manner as the growth of the microcrystals and affords materials with similar morphologies.

Summary

In summary, porphyrin based microcrystals with a variety of morphologies have been synthesized. Simple modification such as reaction temperatures and medium during the synthesis of microcrystals allows for controlled molecular interactions and packing and the resultant morphological diversity of microcrystals. Furthermore, the utilization of surfactant such as CTAB has shown to give a new strategy for microcrystal preparations. The unique properties of the porphyrin building blocks make these microcrystals promising candidates for a wide range of applications in electronics, photonics, and catalytic systems.

Acknowledgments. This work was supported by the Korea Research Foundation (No. 20100015348) and Priority Research Centers Program (NRF20100020209) through the National Research Foundation of Korea (NRF) funded by the Ministry of Education, Science and Technology (MEST).

References

- (a) Chen, J.; Lim, B.; Lee, E. P.; Xia, Y. *Nano Today* **2009**, *4*, 81. (b) Zhang, L.; Webster, T. J. *Nano Today* **2009**, *4*, 66. (c) Zhao, Y.; Jiang, L. *Adv. Mater.* **2009**, *21*, 3621. (d) Shen, J.; Sun, L.-D.; Yan, C.-H. *Dalton Trans.* **2008**, 5687. (e) Liu, Y.; Liu, J. *Acc. Chem. Res.* **2007**, *40*, 315. (f) Teo, B. K.; Sun, X. H. *Chem. Rev.* **2007**, *107*, 1454.
- (a) Zang, L.; Che, Y.; Moore, J. S. *Acc. Chem. Res.* **2008**, *41*, 1596. (b) Laschat, S.; Baro, A.; Steinke, N.; Giesselmann, F.; Hägele, C.; Scalia, G.; Judele, R.; Kapatsina, E.; Sauer, S.; Schreivogel, A.; Tosoni, M. *Angew. Chem. Int. Ed.* **2007**, *46*, 4832.
- (a) Zhang, Y.; Chen, P.; Jiang, L.; Hu, W.; Liu, M. *J. Am. Chem. Soc.* **2009**, *131*, 2756. (b) Briseño, A. L.; Mannsfeld, S. C. B.; Jenekhe, S. A.; Bao, Z.; Xia, Y. *Mater. Today* **2008**, *11*, 38. (c) Cui, S.; Liu, H.; Gan, L.; Li, Y.; Zhu, D. *Adv. Mater.* **2008**, *20*, 2918. (d) Jiang, L.; Fu, Y.; Li, H.; Hu, W. *J. Am. Chem. Soc.* **2008**, *130*, 3937. (e) Tang, M. L.; Reichardt, A. D.; Miyaki, N.; Stoltzberg, R. M.; Bao, Z. *J. Am. Chem. Soc.* **2008**, *130*, 6064.
- (a) Iavicoli, P.; Simon-Sorbed, M.; Amabilino, D. B. *New J. Chem.* **2009**, *33*, 358. (b) Jintoku, H.; Sagawa, T.; Takafuji, M.; Ihara, H. *Org. Biomol. Chem.* **2009**, *7*, 2430. (c) Kojima, T.; Harada, R.; Nakanishi, T.; Kaneko, K.; Fukuzumi, S. *Chem. Mater.* **2007**, *19*, 51. (d) Li, C.; Ly, J.; Lei, B.; Fan, W.; Zhang, D.; Han, J.; Meyya-ppan, M.; Thompson, M.; Zhou, C. *J. Phys. Chem. B* **2004**, *108*, 9646. (e) Schwab, A. D.; Smith, D. E.; Bond-Watts, B.; Johnston, D. E.; Hone, J.; Johnson, A. T.; Paula, J. C. d.; Smith, W. F. *Nano Lett.* **2004**, *4*, 1261. (f) Wang, Z.; Medforth, C. J.; Shelnutt, J. A. *J. Am. Chem. Soc.* **2004**, *126*, 15954. (g) Wang, Z.; Medforth, C. J.; Shelnutt, J. A. *J. Am. Chem. Soc.* **2004**, *126*, 16720. (h) Schwab, A. D.; Smith, D. E.; Rich, C. S.; Young, E. R.; Smith, W. F.; Paula, J. C. D. *J. Phys. Chem. B* **2003**, *107*, 11339.
- (a) Mann, S. *Angew. Chem. Int. Ed.* **2000**, *39*, 3393. (b) Kudora, T.; Irisawa, T.; Ookawa, A. *J. Cryst. Growth* **1977**, *42*, 41. (c) Mullin, J. W. *Crystallization*; Butterworths: London, 1971. (d) Buckley, H. E. *Crystal Growth*; Wiley: New York, 1951. (e) Adair, J. H.; Suvaci, E. *Curr. Opin. Colloid Interface Sci.* **2000**, *5*, 160.
- (a) Lee, S. J.; Mulfort, K. L.; Zuo, X.; Goshe, A. J.; Wesson, P. J.; Nguyen, S. T.; Hupp, J. T.; Tiede, D. M. *J. Am. Chem. Soc.* **2008**, *130*, 836. (b) Lee, S. J.; Cho, S.-H.; Mulfort, K. L.; Tiede, D. M.; Hupp, J. T.; Nguyen, S. T. *J. Am. Chem. Soc.* **2008**, *130*, 16828.
- Lee, S. J.; Jensen, R. A.; Malliakas, C. D.; Kanatzidis, M. G.; Hupp, J. T.; Nguyen, S. T. *J. Mater. Chem.* **2008**, *18*, 3640.
- (a) Medforth, C. J.; Wang, Z.; Martin, K. E.; Song, Y.; Jacobsen, J. L.; Shelnutt, J. A. *Chem. Commun.* **2009**, 7261. (b) Lee, S. J.; Malliakas, C. D.; Kanatzidis, M. G.; Hupp, J. T.; Nguyen, S. T. *Adv. Mater.* **2008**, *20*, 3543. (c) Lee, S. J.; Hupp, J. T.; Nguyen, S. T. *J. Am. Chem. Soc.* **2008**, *130*, 9632. (d) Wang, Z.; Li, Z.; Medforth, C. J.; Shelnutt, J. A. *J. Am. Chem. Soc.* **2007**, *129*, 2440.
- (a) Sendt, K.; Johnston, L. A.; Hough, W. A.; Crossley, M. J.; Hush, N. S.; Reimers, J. R. *J. Am. Chem. Soc.* **2002**, *124*, 9299. (b) Hunter, C. A.; Sanders, J. K. M.; Stone, A. J. *Chem. Phys.* **1989**, *133*, 395.
- (a) Auvray, X.; Petipas, C.; Anthore, R.; Rico, I.; Lattes, A. *J. Phys. Chem.* **1989**, *93*, 7458. (b) Hakemi, H.; Varanasi, P. P.; Tcheurekdjian, N. *J. Phys. Chem.* **1987**, *91*, 120.